



Universiteit  
Leiden

The Netherlands

## Improving diagnostic, prognostic and predictive biomarkers in colorectal cancer: the role of proteomics and stromatogenesis

Huijbers, A.

### Citation

Huijbers, A. (2022, June 2). *Improving diagnostic, prognostic and predictive biomarkers in colorectal cancer: the role of proteomics and stromatogenesis*. Retrieved from <https://hdl.handle.net/1887/3307244>

Version: Publisher's Version

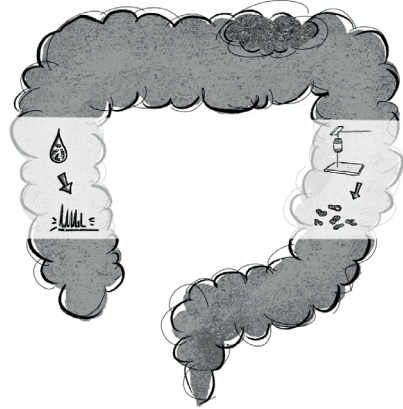
License: [Licence agreement concerning inclusion of doctoral thesis in the Institutional Repository of the University of Leiden](#)

Downloaded from: <https://hdl.handle.net/1887/3307244>

**Note:** To cite this publication please use the final published version (if applicable).



# 6



Unravelling the tumor associated stroma in colon cancer patients using laser capture microdissection and reverse phase protein microarray.

A. Huijbers  
G.W. van Pelt  
E. Pin  
M. Pierobon  
C. Belluco  
L. Liotta  
E. Petricoin  
R.A.E.M. Tollenaar  
W.E. Mesker

Submitted

## **ABSTRACT**

### **Introduction**

The tumor microenvironment is an important target for cancer therapy. The prognostic value of the tumor-stroma ratio in colon cancer patients is well described. In order to evaluate the contribution of the underpinning signalling and molecular architecture of the tumor associated stroma to the aggressive stroma-high phenotype, we utilized laser capture microdissection coupled to broad-scale protein pathway activation mapping using reverse phase protein microarrays.

### **Material and Methods**

Patients with histologically proven stage II and stage III colon cancer were selected from the LUMC database. Hematoxylin and Eosin (H&E) stained sections from the most invasive part of the primary tumor were scored for the tumor-stroma ratio. Reverse phase protein microarray was performed using micro-dissected material to generate multiplexed pathway profiling. For each sample, 58 endpoints were analysed.

### **Results**

Comparison of the 58 endpoints in 30 colon cancer patients (15 stroma-high and 15 stroma-low) showed that phosphorylation of VEGFR-2 was significantly higher in the stroma-high group compared to the stroma-low group ( $p=0.02$ ) and that ZAP70, eNOS and ICAM-1 was significantly lower in the stroma-high group ( $p=0.01$ ,  $p=0.04$  and  $p=0.03$ , respectively). Correlation analysis showed a major eNOS node with many interconnections in the tumor stroma within the stroma-low group.

### **Conclusion**

This pilot study showed the potential presence of biochemical derangements in the tumor stroma of tumors from patients with aggressive colon (stroma-high) cancer with increased activation of VEGFR-2 and decreased activation of ZAP70, eNOS and ICAM-1. Focusing on the stroma-low group, there is a significantly higher expression of eNOS with many interconnections including ARPC2. These interconnections may contribute to the better behaviour of the stroma-low tumors.

## INTRODUCTION

The tumor microenvironment, and especially the stroma surrounding the tumor cells, is an important target for cancer therapy. Tumor stroma plays an important role in tumorigenesis. From initiation to invasion and metastasis, tumor stroma interacts with both malignant and non-malignant cells.

Tumor stroma is composed of a mixture of cells, including immune cells, fibroblasts and endothelial cells, that are embedded in the proteins of the extracellular matrix (ECM). When the ECM interacts with the tumor cells, it will influence disease progression and metastatic capacity. One of the most important cell types of the tumor stroma is the activated form of fibroblasts, the so-called cancer-associated fibroblasts (CAFs). CAFs are involved in tumor progression and invasion. Stromal cells stimulate blood vessel formation and supply the tumor with growth factors, cytokines and metabolites [1]. This might explain the decreased survival time for patients with a tumor with high stromal content.

Tumor-stroma ratio (TSR) distinguishes between aggressive and non-aggressive tumors. The prognostic value of TSR is well described and validated [2-4]. Colon cancer patients with a high (>50%) amount of intratumor stroma have a poor prognosis compared to patients with a low amount ( $\leq$ 50%) [2-5]. The TSR is easily determined on conventional hematoxylin and eosin (H&E) stained tissue sections used for routine pathological investigation. Moreover, in breast and esophageal cancer, this prognostic parameter has also been validated in large patient series [6-10]. Furthermore, in other types of epithelial cancer (for example cervical, prostate, bladder, head/neck and lung cancer), the same prognostic value was found by different international research groups [11-17].

However, it is not yet entirely clear why TSR makes this distinction between aggressive and non-aggressive tumors since the underlying mechanism is still not fully understood. Nevertheless, we do know that tumor stroma plays an important role in tumor formation and progression [18]. A colon tumor with a high stromal content has a highly increased interaction between tumor and stromal cells. Specific molecular changes in colon cancer cells cause the recruitment and activation of surrounding stromal cells, which enables tumor progression by releasing soluble growth factors, metabolites and cytokines [18].

In order to evaluate the contribution of the underpinning signalling and molecular architecture of the tumor associated stroma to the aggressive stroma-high pheno-

type, we utilized laser capture microdissection (LCM) coupled to broad-scale protein pathway activation mapping using reverse phase protein microarrays (RPMA). This technique uses cellular enrichment of specific tissue cells via LCM for tissue biomarker discovery and selection criteria for personalized treatment [20-23]. RPMA is a high throughput multiplex proteomic platform. It has the ability to measure hundreds of analytes in a large number of samples with only a small amount of biological material [24-26]. By focusing on activation in terms of phosphorylation, next to kinase expression, this technique has been successful for signalling network analysis [27-30]. Such analysis could identify new stromal-based targeted information interesting for treatment options through the identification of activated pathways within the tumor stroma of patients with aggressive colon cancer.

## **MATERIAL & METHODS**

### **Patients**

Patients with histologically proven stage II and stage III colon cancer were selected from the Leiden University Medical Center (LUMC, The Netherlands) database. All patients underwent surgical resection of the primary tumor between 2001 and 2011, with or without adjuvant chemotherapy. Only patients whose fresh frozen tumor material was available were selected. Patients who received neo-adjuvant treatment were excluded.

### **Histopathological scoring**

By using conventional microscopy, H&E stained sections from the most invasive part of the primary tumor were scored for the amount of stroma. TSR was defined as the percentage intra-tumor stroma tissue relative to the neoplastic cell component. The protocol for TSR scoring has been described previously [2, 31]. In short, the most invasive tumor area with the highest amount of stroma on each slide was selected using a 2.5x or 5x objective. Using a 10x objective areas where tumor cells are present at all borders of the image field were scored. Scoring percentages were given per tenfold (10, 20, 30% etc.) per image-field (Figure 1). When mucinous tissue was present within a field that matched our scoring criteria, the mucinous tissue was visually excluded for the scoring. Two investigators (GvP, AH) estimated the stromal percentage in a blinded manner. In case of discrepancy slides were reviewed to reach consensus. In case no consensus could be reached a third observer was decisive (WM). Patients were categorized into two groups; a stroma-high (>50% stroma) and a stroma-low (= $<$ 50% stroma) group.

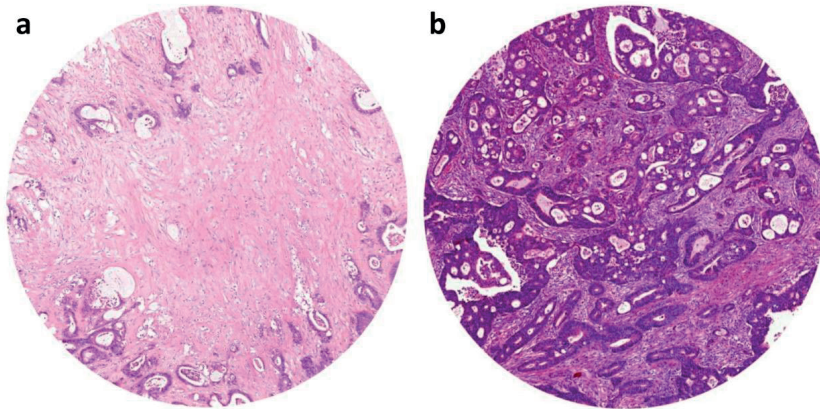


**Figure 1.** Examples of stroma-high (a) and stroma-low (b) haematoxylin and eosin (H&E) stained paraffin sections at the most invasive part of primary colon cancers (100x magnification).

### Laser capture microdissection (LCM)

As described previously, highly enriched stromal cell subpopulations were obtained using Arcturus Veritas 704 LCM System (Arcturus, Mountain View, CA USA) [32, 33] (Figure 2). Stroma cells were captured when they were surrounded by tumor epithelium cells on all four corners of microscopic field with a magnification of 20x and the stroma was in direct contact with the external edge of the tumor. Lymphocyte agglomerates, when present, were not captured. Microdissected material was stored at  $-80^{\circ}\text{C}$  and cell lysates were prepared for RPMA as previously described [28, 34].

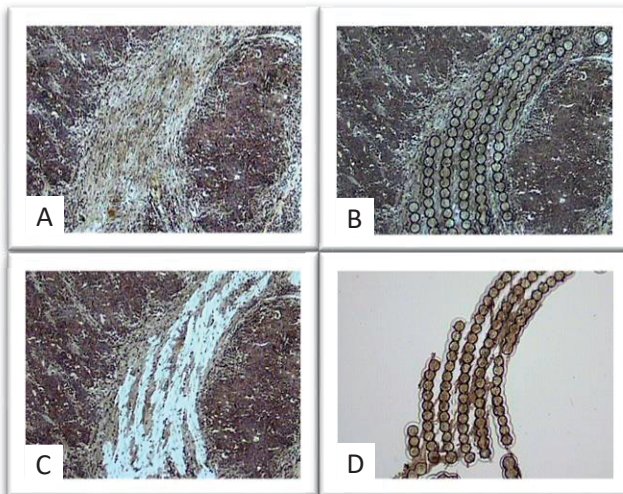


**Figure 2.** Laser capture images from tumor associated stroma cells before and after LCM.  
 A) Inter tumor stroma area microscopically selected. B) Selected tumor stroma tissue by laser capture. C) After laser capture. D) Removed stroma tissue for analysis on a nitrocellulose membrane.

## Reverse phase protein microarray analysis (RPMA)

Cell lysates were printed in triplicate onto nitrocellulose coated slides Using a 2470 Aushon Arrayer (Aushon BioSystems, Billerica, MA, USA) along with standard curves for quality assurance (Grace BioLabs, Bend, OR, USA). A complete list of all 58 proteins and phosphoproteins measured in this study are listed in table 2. These analytes were chosen based on their involvement in key aspects of epithelial mesenchymal transition, ECM composition and remodeling, angiogenesis, inflammation and transcription. All antibodies used in these studies were validated by western blotting for single band specificity prior to use [35-38]. Immunostaining was performed as previously described [34]. Concisely, each slide was incubated with one primary antibody targeting the protein of interest. As secondary antibodies biotinylated goat anti-rabbit (1:7,500, Vector Laboratories Inc, Burlingame, CA) and rabbit anti-mouse (1:10, DakoCytomation, Carpinteria, CA, USA) IgG were used. Using a tyramide-based avidin/ biotin amplification system (DakoCytomation, Carpinteria, CA, USA) coupled with Streptavidin conjugated IRDye 680 (LI-COR, Lincoln, NE, USA) signal amplification and detection were achieved. Total protein was measured following manufacturing instructions using a Sypro Ruby protein blot staining protocol (Molecular Probes, Eugene, OR, USA). With a Tecan PowerScanner (Tecan, Männedorf, Switzerland) images were acquired and analyzed with the MicroVigene software Version 5.1.0.0 (Vigenetech, Carlisle, MA, USA) [34].

**Table 1.** Patient characteristics

|                                    | Total      |    | Stroma-low |    | Stroma-high |    | P-value |
|------------------------------------|------------|----|------------|----|-------------|----|---------|
|                                    | N = 30     | %  | N = 15     | %  | N = 15      | %  |         |
| <b>Age</b> (median in yrs [range]) | 67 [38-90] |    | 70 [58-90] |    | 64 [38-79]  |    | 0.47    |
| <b>Gender</b>                      |            |    |            |    |             |    |         |
| Female                             | 14         | 47 | 8          | 53 | 6           | 40 | 0.46    |
| Male                               | 16         | 53 | 7          | 47 | 9           | 60 |         |
| <b>Tumor Location</b>              |            |    |            |    |             |    |         |
| Left-sided                         | 14         | 47 | 7          | 47 | 7           | 47 | 1.00    |
| Right-sided                        | 16         | 53 | 8          | 53 | 8           | 53 |         |
| <b>T-stage</b>                     |            |    |            |    |             |    |         |
| T3                                 | 26         | 87 | 13         | 87 | 13          | 87 | 1.00    |
| T4                                 | 4          | 13 | 2          | 13 | 2           | 13 |         |
| <b>N-stage</b>                     |            |    |            |    |             |    |         |
| N0                                 | 11         | 37 | 9          | 60 | 2           | 13 | 0.02    |
| N1                                 | 8          | 27 | 4          | 27 | 4           | 27 |         |
| N2                                 | 11         | 37 | 2          | 13 | 9           | 60 |         |
| <b>TNM Stage</b>                   |            |    |            |    |             |    |         |
| II                                 | 11         | 37 | 9          | 60 | 2           | 13 | 0.01    |
| III                                | 19         | 63 | 6          | 40 | 13          | 87 |         |
| <b>Adjuvant therapy</b>            |            |    |            |    |             |    |         |
| No                                 | 19         | 63 | 12         | 80 | 7           | 47 | 0.06    |
| Yes                                | 11         | 37 | 3          | 20 | 8           | 53 |         |

**Table 2.** All 58 endpoints analysed with reverse phase protein microarray analysis (RPMA) sorted by group.

| 58 endpoints analyzed by RPMA   |  |   |
|---|--|---|
| <b>Growth factors and receptors</b><br><b>VEGFR2 (Y1175)</b> SD<br><b>PDGFR</b> TTS<br>PDGFRbeta (Y751)<br>IGF I<br><b>IGF I R (Y1135-36)/IR (Y1150-51)</b> TTS<br>TGFbeta<br>NGF<br><b>Wnt5a/b</b> TTS | <b>Protein Kinases</b><br>Jak 1 (Y1022-23)<br>Jak 2 (Y1007-8)<br><b>Zap70 (Y319)/Syk (Y352)</b> SD<br>Akt (S473)<br>Erk 1/2 (T202-Y204)<br>FAK<br>FAK (Y576-577)<br>IRAK I<br>p38MAPK (T180-Y182)<br><b>Lck (Y505)</b> TTS | <b>EM Composition</b><br>Collagen I<br><br><b>Fibroplastic component</b><br><b>FSP/S100A4</b> TTS<br>alphaSMA<br><br><b>Inflammatory component</b><br>CD45<br>CD5L<br>Arpc2 |
| <b>Interleukins</b><br>IL6<br>IL10<br>IL1 beta<br>IL8   | <b>Downstreams</b><br>SMAD 4<br>SMAD 1/5/8<br>Stat4 (Y693)<br>Stat6 (Y641)<br>Stat1 (Y701)<br>Stat3 (Y705)<br><b>Stat5 (Y694)</b> TTS<br>Beta Catenin (T41-S45)<br>DKK I<br><b>eNOS (S113)</b> SD<br>eNOS/NOSIII (S116)    | <b>Transcription factors</b><br>NFkB.p65.S536<br>Egr I  |
| <b>EMT and EM remodelling</b><br>Vimentin<br>E-Cadherin<br>Twist I<br><b>MMP2</b> TTS<br>MMP9<br>MMP14<br>TIMP2<br>TIMP3  |  | <b>Other markers</b><br>CAV I<br>CAV I (Y14)<br><b>ICAM I</b> SD<br>cILAMINA<br>SERPINA I<br>Cox2<br>OPN<br>Podoplanin<br>LDHA  |
| <b>Legend:</b><br>SD = statistically different<br>TTS = a trend towards significance (0.05 < p < 0.1)   |  |   |

SD meaning statistically different between the stroma-high and stroma-low groups (p-value <0.05). TTS meaning a trend towards significance with a p-value between 0.05 and 0.1.

## Data analysis

To explore the changes in the activation/phosphorylation and expression levels of different analytes mean comparison was used. A two-sample t-test was used for analytes that were normally distributed. For proteins/phosphoproteins presenting with asymmetric distribution the Wilcoxon rank sum test was performed. Data analysis was performed using SPSS version 19. All p values < 0.05 were considered statistically significant. To explore the interactions between proteins/phosphoproteins within the cellular compartments Spearman Rho correlation coefficients were calculated. Correlation maps were created with Gephi version 0.8.2. Only associations with a correlation coefficient  $\geq 0.75$  were included in the correlation maps.

## RESULTS

The LUMC database consisted of 80 patients whose TSR could be scored and fresh frozen tissue was available. For this feasibility study, only cases with  $\leq 30\%$  stroma or  $\geq 70\%$  stroma were analysed. A total of 30 colon cancer samples (15 stroma-high and 15 stroma-low) were randomly selected from patients with histologically proven stage II and stage III colon cancer. The amount of stroma in the frozen tissue sample was double checked to be the same as the paraffin sample before including for analysis. Eleven patients were TNM stage II (37%) and 19 patients TNM stage III (63%). For detailed patient characteristics, see table 1.

Mean comparison analysis showed that 4 of the 58 analytes measured were statistically different between the two stroma groups. Phosphorylation of vascular endothelial growth factor receptor-2 (VEGFR-2) was significantly higher in the stroma-high group compared to the stroma-low group ( $p=0.02$ ). Furthermore, zeta-chain-associated protein kinase 70 (ZAP70), endothelial nitric oxide synthase (eNOS) and intercellular adhesion molecule-1 (ICAM-1) were significantly lower in the stroma-high group compared to the stroma-low group ( $p=0.01$ ,  $p=0.04$  and  $p=0.03$ , respectively) (Figure 3).

Correlation analysis demonstrated more interconnections in the stroma-low group compared to the stroma-high group where proteins did not seem to trend together. When the analysis was limited to highly correlated pairs ( $\geq 0.75$ ), some major clusters were identified (Figure 4). The stroma-low group showed to have two major nodes: eNOS and ARPC2 correlated pairs, respectively.

## DISCUSSION

These results reveal the potential presence of biochemical derangements in the tumor stroma of tumors from patients with aggressive colon cancer with increased activation of VEGFR-2 and decreased activation of ZAP70, ICAM-1 and eNOS.

First, VEGFR-2 is one of the most prominent ligand-receptor complexes in the VEGF system. It can lead to endothelial cell proliferation, migration, survival and new vessel formation involved in angiogenesis [39]. High levels of VEGF expression are related to poorer survival and an increased rate of distant metastases in colorectal cancer patients [40]. To find altered levels of VEGFR in stroma-high patients correlates well

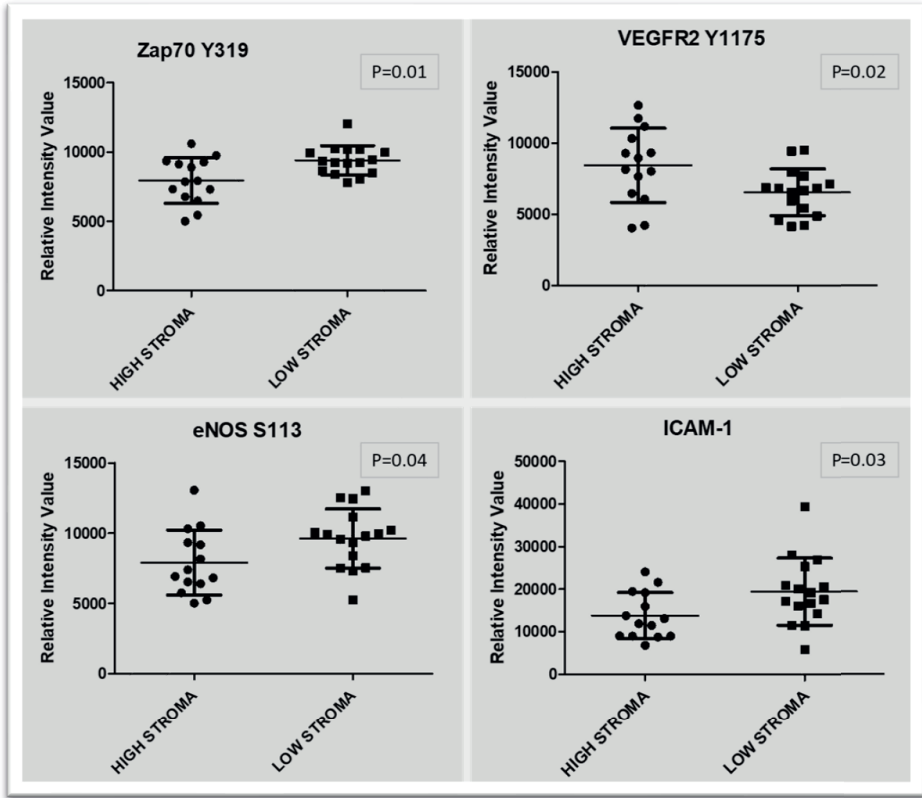
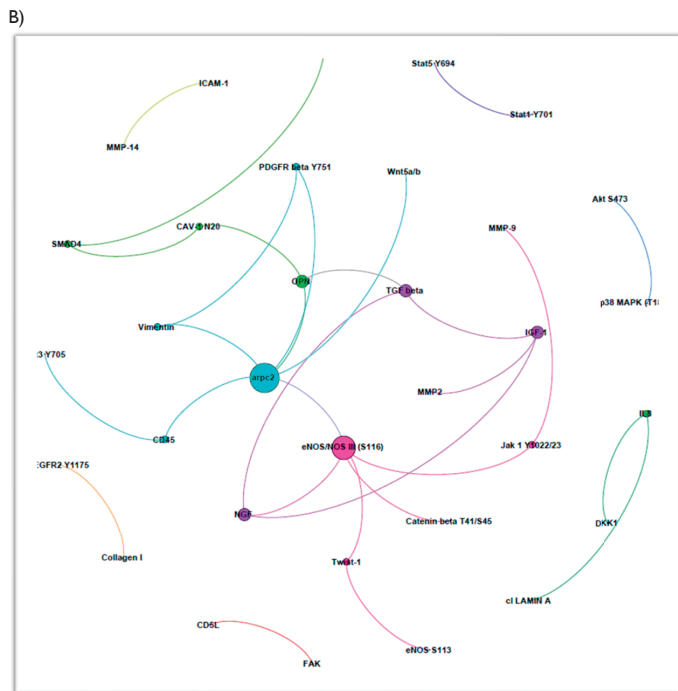
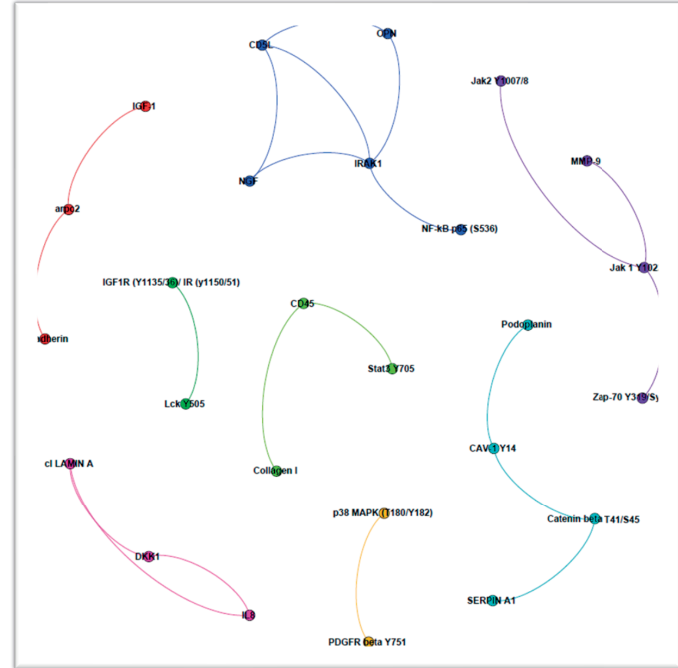


Figure 3. Significantly different analytes in stroma-high versus stroma-low group.

with the poorer survival of this group and could be an extra linking factor for new therapeutic strategies.

Considering the central role VEGFR plays in angiogenesis and cell migration, the results could suggest that anti-VEGFR targeted therapy could be considered for a pre-stratified group of patients with aggressive tumors with high recurrence rates. The Quick and Simple and Reliable trial (QUASAR2), is a phase III randomized trial of adjuvant capecitabine (CAP)  $\pm$  bevacizumab (BEV) after complete surgical resection of high-risk stage II and stage III colorectal cancer [41]. Bevacizumab is a recombinant humanized monoclonal antibody that blocks angiogenesis by inhibiting vascular endothelial growth factor A (VEGF-A). VEGF-A is a growth factor protein that stimulates angiogenesis in a variety of diseases, especially in cancer. In this study, our group investigated whether this anti-angiogenic therapy might improve survival of patients with a stroma-high profile with a higher expression of VEGFR-2 and potentially increased angiogenesis. However, no benefit was found in response to treatment with

**Figure 4.** Correlation maps showing protein interactions and networks within the tumor stroma for a) for stroma-high and b) stroma-low samples. Only correlations with a coefficient  $\geq 0.75$  are shown in the maps.



bevacizumab when stratified for TSR [5]. Assessing different angiogenetic strategies and therapeutic options could have an additional value for improving survival of the stroma-high patient population.

Second, ZAP70 encodes an enzyme belonging to the protein tyrosine kinase family and plays a role in T-cell development and lymphocyte activation. It is used as a prognostic marker in identifying different forms of chronic lymphocytic leukaemia (CLL), where the expression of ZAP70 is associated with a significantly lower overall survival [42]. There is currently no available data on its role in CRC. In our study, we found a lower expression of ZAP70 in the stroma-high group. This correlates with our visual finding that stroma-high tumors have microscopically less lymphocytic infiltration compared to the stroma-low tumors. Further research is necessary to unravel the underlying mechanism and the possible clinical implications behind this.

Third ICAM-1 is a surface glycoprotein and is known to be a member of the immunoglobulin gene superfamily of adhesion molecules. It is expressed on vascular endothelium and plays a key role in the trans-endothelial migration of neutrophils and T-cell activation [43]. It has been suggested that ICAM-1 can inhibit cancer progression by activation of the host immune surveillance system by adherence to the extracellular matrix and thereby alleviating or eliminating metastasis of CRC [43, 44]. In our study, a lower expression of ICAM-1 was seen in the stroma-high population, correlating with a worse prognosis.

Lastly, eNOS is a gene expressed in the endothelium involved in the production of nitric oxide (NO), which plays a central role in maintaining endothelial cell functional integrity, regulating hemodynamics, and establishing collateral circulation [45]. Literature suggests that NO plays a key role in physiological regulations, including defence mechanisms against infectious disease and tumors [46]. A high level of expression of endothelial cell nitric oxide synthase (eNOS) in micro vessels in the tumor-adjacent area protects against tumor metastasis [47]. In our study, a higher expression was seen in the stromal tissue of the stroma-low group with better survival rates, correlating with this hypothesis.

While the four above discussed analytes are differently expressed among different groups, we also performed a correlation analysis (see correlation map in Figure 4). This correlation analysis showed that in addition to those detected differences, eNOS is a node that shows many interconnections in the tumor stroma within the stroma-low group. With the characteristics of eNOS as described above, it may be an important

analyte to contribute to the better prognosis of patients with a stroma-low tumor compared to the stroma-high group.

The other lead in the correlation map within the stroma-low group is ARPC2. Literature shows that ARPC2 in gastric cancers showed significant associations with large tumor size, lymph node invasion, and high tumor stage. In addition, in the same study, ARPC2-positive patients had lower recurrent free and overall free survival rates compared to ARPC2-negative patients [48]. Regarding breast cancer, ARPC2 is described to promote cancer proliferation and metastasis [49]. For colon cancer, literature so far only described an under-expression of ARPC2 in early colorectal cancer [50]. In our study, ARPC2 is equally expressed in the stroma-high and stroma-low group. However, ARPC2 shows many correlations and might be an important part of the stroma-low micro-environment network.

This pilot study showed the potential presence of biochemical derangements in the tumor stroma of tumors from patients with aggressive colon cancer with increased activation of VEGFR-2 and decreased activation of ZAP70, ICAM-1 and eNOS. Moreover, by focusing on the stroma-low group instead of the stroma-high group, there is a significantly higher expression of eNOS with many interconnections including ARPC2. These interconnections may play an important contribution to the prognosis of the stroma-low group. The preliminary findings in our study may offer a new lead for additional research to better understand the different tumor phenotypes of these two prognostically different groups based on their stroma amount.

## REFERENCE LIST

1. van Pelt, G.W., et al., The tumour-stroma ratio in colon cancer: the biological role and its prognostic impact. *Histopathology*, 2018. 73(2): p. 197-206.
2. Mesker, W.E., et al., The carcinoma-stromal ratio of colon carcinoma is an independent factor for survival compared to lymph node status and tumor stage. *Cell Oncol*, 2007. 29(5): p. 387-98.
3. Huijbers, A., et al., The proportion of tumor-stroma as a strong prognosticator for stage II and III colon cancer patients: validation in the VICTOR trial. *Ann Oncol*, 2013. 24(1): p. 179-85.
4. Mesker, W.E., et al., Presence of a high amount of stroma and downregulation of SMAD4 predict for worse survival for stage I-II colon cancer patients. *Cell Oncol*, 2009. 31(3): p. 169-78.
5. Huijbers, A., et al., The value of additional bevacizumab in patients with high-risk stroma-high colon cancer: A study within the QUASAR2 trial, an open-label randomized phase 3 trial. *J Surg Oncol*, 2018. 117(5): p. 1043-1048.
6. de Kruijf, E.M., et al., Tumor-stroma ratio in the primary tumor is a prognostic factor in early breast cancer patients, especially in triple-negative carcinoma patients. *Breast Cancer Res Treat*, 2011. 125(3): p. 687-96.
7. Dekker, T.J., et al., Prognostic significance of the tumor-stroma ratio: validation study in node-negative premenopausal breast cancer patients from the EORTC perioperative chemotherapy (POP) trial (10854). *Breast Cancer Res Treat*, 2013. 139(2): p. 371-9.
8. Gujam, F.J., et al., The relationship between the tumour stroma percentage, clinicopathological characteristics and outcome in patients with operable ductal breast cancer. *Br J Cancer*, 2014. 111(1): p. 157-65.
9. Moorman, A.M., et al., The prognostic value of tumour-stroma ratio in triple-negative breast cancer. *Eur J Surg Oncol*, 2012. 38(4): p. 307-13.
10. Courrech Staal, E.F., et al., The stromal part of adenocarcinomas of the oesophagus: does it conceal targets for therapy? *Eur J Cancer*, 2010. 46(4): p. 720-8.
11. Liu, J., et al., Tumor-stroma ratio is an independent predictor for survival in early cervical carcinoma. *Gynecol Oncol*, 2014. 132(1): p. 81-6.
12. Lv, Z., et al., Tumor-stroma ratio is a prognostic factor for survival in hepatocellular carcinoma patients after liver resection or transplantation. *Surgery*, 2015. 158(1): p. 142-50.
13. Wang, K., et al., Tumor-stroma ratio is an independent predictor for survival in esophageal squamous cell carcinoma. *J Thorac Oncol*, 2012. 7(9): p. 1457-61.
14. Wang, Z., et al., [Tumor-stroma ratio is an independent prognostic factor of non-small cell lung cancer]. *Zhongguo Fei Ai Za Zhi*, 2013. 16(4): p. 191-6.
15. Zhang, T., et al., Tumor-stroma ratio is an independent predictor for survival in NSCLC. *Int J Clin Exp Pathol*, 2015. 8(9): p. 11348-55.
16. Zhang, X.L., et al., The tumor-stroma ratio is an independent predictor for survival in nasopharyngeal cancer. *Oncol Res Treat*, 2014. 37(9): p. 480-4.
17. Pongsuvareeyakul, T., et al., Prognostic evaluation of tumor-stroma ratio in patients with early stage cervical adenocarcinoma treated by surgery. *Asian Pac J Cancer Prev*, 2015. 16(10): p. 4363-8.
18. Augsten, M., et al., A digest on the role of the tumor microenvironment in gastrointestinal cancers. *Cancer Microenviron*, 2010. 3(1): p. 167-76.
19. Calon, A., et al., Dependency of colorectal cancer on a TGF-beta-driven program in stromal cells for metastasis initiation. *Cancer Cell*, 2012. 22(5): p. 571-84.
20. Silvestri, A., et al., Individualized therapy for metastatic colorectal cancer. *J Intern Med*, 2013. 274(1): p. 1-24.

21. Pierobon, M., et al., Application of molecular technologies for phosphoproteomic analysis of clinical samples. *Oncogene*, 2015. 34(7): p. 805-14.
22. Zupa, A., et al., A pilot characterization of human lung NSCLC by protein pathway activation mapping. *J Thorac Oncol*, 2012. 7(12): p. 1755-1766.
23. Jameson, G.S., et al., A pilot study utilizing multi-omic molecular profiling to find potential targets and select individualized treatments for patients with previously treated metastatic breast cancer. *Breast Cancer Res Treat*, 2014. 147(3): p. 579-88.
24. Pierobon, M., et al., Pilot phase I/II personalized therapy trial for metastatic colorectal cancer: evaluating the feasibility of protein pathway activation mapping for stratifying patients to therapy with imatinib and panitumumab. *J Proteome Res*, 2014. 13(6): p. 2846-55.
25. Paweletz, C.P., et al., Reverse phase protein microarrays which capture disease progression show activation of pro-survival pathways at the cancer invasion front. *Oncogene*, 2001. 20(16): p. 1981-9.
26. VanMeter, A., et al., Reverse-phase protein microarrays: application to biomarker discovery and translational medicine. *Expert Rev Mol Diagn*, 2007. 7(5): p. 625-33.
27. Wulfskuhle, J.D., et al., Molecular analysis of HER2 signaling in human breast cancer by functional protein pathway activation mapping. *Clin Cancer Res*, 2012. 18(23): p. 6426-35.
28. Baldelli, E., et al., Functional signaling pathway analysis of lung adenocarcinomas identifies novel therapeutic targets for KRAS mutant tumors. *Oncotarget*, 2015. 6(32): p. 32368-79.
29. Baldelli, E., et al., Impact of upfront cellular enrichment by laser capture microdissection on protein and phosphoprotein drug target signaling activation measurements in human lung cancer: Implications for personalized medicine. *Proteomics Clin Appl*, 2015. 9(9-10): p. 928-37.
30. Federici, G., et al., Systems analysis of the NCI-60 cancer cell lines by alignment of protein pathway activation modules with "-OMIC" data fields and therapeutic response signatures. *Mol Cancer Res*, 2013. 11(6): p. 676-85.
31. van Pelt, G.W., et al., Scoring the tumor-stroma ratio in colon cancer: procedure and recommendations. *Virchows Arch*, 2018. 473(4): p. 405-412.
32. Espina, V., et al., Laser capture microdissection. *Methods Mol Biol*, 2006. 319: p. 213-29.
33. Pin, E., et al., A pilot study exploring the molecular architecture of the tumor microenvironment in human prostate cancer using laser capture microdissection and reverse phase protein microarray. *Mol Oncol*, 2016. 10(10): p. 1585-1594.
34. Pin, E., G. Federici, and E.F. Petricoin, 3rd, Preparation and use of reverse protein microarrays. *Curr Protoc Protein Sci*, 2014. 75: p. Unit 27 7.
35. Van Meter, M.E., et al., K-RasG12D expression induces hyperproliferation and aberrant signaling in primary hematopoietic stem/progenitor cells. *Blood*, 2007. 109(9): p. 3945-52.
36. Speer, R., et al., Development of reverse phase protein microarrays for clinical applications and patient-tailored therapy. *Cancer Genomics Proteomics*, 2007. 4(3): p. 157-64.
37. Speer, R., et al., Reverse-phase protein microarrays for tissue-based analysis. *Curr Opin Mol Ther*, 2005. 7(3): p. 240-5.
38. Espina, V., et al., Protein microarrays: molecular profiling technologies for clinical specimens. *Proteomics*, 2003. 3(11): p. 2091-100.
39. Abhinand, C.S., et al., VEGF-A/VEGFR2 signaling network in endothelial cells relevant to angiogenesis. *J Cell Commun Signal*, 2016. 10(4): p. 347-354.
40. Cho, T., et al., The role of microvessel density, lymph node metastasis, and tumor size as prognostic factors of distant metastasis in colorectal cancer. *Oncol Lett*, 2017. 13(6): p. 4327-4333.

41. Kerr, R.S., et al., Adjuvant capecitabine plus bevacizumab versus capecitabine alone in patients with colorectal cancer (QUASAR 2): an open-label, randomised phase 3 trial. *Lancet Oncol*, 2016. 17(11): p. 1543-1557.
42. Cramer, P. and M. Hallek, Prognostic factors in chronic lymphocytic leukemia-what do we need to know? *Nat Rev Clin Oncol*, 2011. 8(1): p. 38-47.
43. Hubbard, A.K. and R. Rothlein, Intercellular adhesion molecule-1 (ICAM-1) expression and cell signaling cascades. *Free Radic Biol Med*, 2000. 28(9): p. 1379-86.
44. Wang, Q.L., et al., Polymorphisms of the ICAM-1 exon 6 (E469K) are associated with differentiation of colorectal cancer. *J Exp Clin Cancer Res*, 2009. 28: p. 139.
45. Fukumura, D., et al., Predominant role of endothelial nitric oxide synthase in vascular endothelial growth factor-induced angiogenesis and vascular permeability. *Proc Natl Acad Sci U S A*, 2001. 98(5): p. 2604-9.
46. Zhao, Y., P.M. Vanhoutte, and S.W. Leung, Vascular nitric oxide: Beyond eNOS. *J Pharmacol Sci*, 2015. 129(2): p. 83-94.
47. Mortensen, K., et al., High expression of endothelial cell nitric oxide synthase in peritumoral microvessels predicts increased disease-free survival in colorectal cancer. *Cancer Lett*, 2004. 216(1): p. 109-14.
48. Zhang, J., et al., Role of ARPC2 in Human Gastric Cancer. *Mediators Inflamm*, 2017. 2017: p. 5432818.
49. Cheng, Z., et al., ARPC2 promotes breast cancer proliferation and metastasis. *Oncol Rep*, 2019. 41(6): p. 3189-3200.
50. Lau, T.P., et al., Pair-wise comparison analysis of differential expression of mRNAs in early and advanced stage primary colorectal adenocarcinomas. *BMJ Open*, 2014. 4(8): p. e004930.